CHEMICAL ENGINEERING TRANSACTIONS
VOL. 66, 2018
A publication of AIDIC
The Italian Association of Chemical Engineering
Online at www.aidic.it/cet
Guest Editors: Songying Zhao, Yougang Sun, Ye Zhou

ISBN 978-88-95608-63-1; **ISSN** 2283-9216
DOI: 10.3303/CET1866068

Convective Heat Transfer Flow of Nanofluid in an Isosceles Triangular Shaped Enclosure with an Uneven Bottom Wall

Md. Jashim Uddin*, A. K. M. Fazlul Hoque

Faculty of Science and Information Technology, Daffodil International University, Dhaka, Bangladesh
jashim.fluidm@gmail.com,

The aim of this study is to investigate the convective flow of nanofluids inside an isosceles triangular shaped enclosure with the uneven bottom wall using nonhomogeneous dynamic model. The inclined walls of the enclosure are maintained at constant low temperature. The uniform thermal boundary condition has been considered at the bottom wall. The enclosure is permeated by a uniform magnetic field. The Galerkin weighted residual finite element method has been employed to solve the governing nonlinear equations. The copper oxide-water nanofluid has been taken to gain insight into the flow and thermal fields of nanofluids. The heat transfer rate for different flow parameters of the problem has been calculated. The result shows that the flow and thermal field are strongly controlled by the applied magnetic field. The heat transfer rate is an increasing function of nanoparticle volume fraction, thermal Rayleigh number and magnetic field inclination angle whereas it is a decreasing function of the nanoparticle diameter and the Hartmann number.

1. Introduction

The research on solar thermal collector is an important research topic due to its importance in using solar energy. The solar thermal collector has a wide range of applications. As for example, it is using in solar cooling system, solar dryer, solar desalination, solar home system, solar water heating system, and so on. Nowadays, different shapes of the solar thermal accumulator are accessible commercially. However, research is still going on to find the true shape and design where heat transfer rate is maximum. The major aspects of solar thermal technology are to achieve the highest heat transfer rate in applications.

Convection mode of heat transfer has been given a mammoth importance by different investigators in several shapes of solar thermal collectors or enclosures. The buoyancy drove convection happens in a great number of industrial applications such as indoor ventilation, radiators, cooling reactors, electrical, electronic components, solar thermal collectors, heat exchangers and so on (Tzeng et al., 2005). However, the conventional fluid such as air, water, ethylene glycol, kerosene etc. used in different applications, cannot fulfill the demand where the higher thermal conductivity is needed. Many researches show that the implementation of nanofluids can overcome the barriers in heat transfer and engineering applications. The evidence of higher heat transfer rate has been calculated using nanofluids (Wen and Ding, 2004). Nanofluid is prepared by base fluid and nanoparticles (Haichao et al., 2017; Ting and Jianhong, 2017). A comprehensive literature review on heat transfer rate of nanofluids can be found in Uddin et al. (2016a). Lai and Yang (2011) inspected the heat transfer rate of alumina-water nanofluid filled square enclosure. Results indicated that the average Nusselt number surges with the upsurge of Rayleigh number and the amount of nanoparticle. Tiwari and Das (2007) scrutinized the heat transfer intensification in square cavity using nanofluids. They found that the directions of the moving walls of the cavity controls the flow and heat transfer rate whereas Ghasemi and Aminossadati (2010) have shown that nanofluid improves the cooling performance at low thermal Rayleigh number. Also, Bondareva et al. (2015) reported results on convection for a triangular cavity using nanofluids and found that the triangular cavity plays a significant role in enhancing heat transfer rate. Uddin et al. (2017b) have studied the heat transfer flow in a homocentric annulus filled with nanofluid and showed that the heat transfer rate is decreased by reducing the diameter of the nanoparticles. They have given importance on Brownian motion effects. Billah et al. (2013) studied the heat transfer enhancement of nanofluids in an inclined triangular enclosure. It is shown that the variation of the average Nusselt number is linear with the solid volume fraction.

Please cite this article as: Uddin M.J., Hoque A.K.M.F., 2018, Convective heat transfer flow of nanofluid in an isosceles triangular shaped enclosure with an uneven bottom wall, Chemical Engineering Transactions, 66, 403-408 DOI:10.3303/CET1866068

Recently, using dynamic nonhomogeneous model, Uddin et al. (2016b, 2017a, 2017b, 2017c) have studied the heat transfer rate in nanofluids filled different shapes of enclosures. They have shown the uniform levels of concentration are obtained for 1-20 nm diameter of nanoparticles. The better heat transfer coefficients are calculated and compared with experimental investigations in their studies.
Therefore, triangular shape enclosure is important in the practical applications. Also, in light of many advantages of nanofluids, different types of solar collector have been studied (Colangelo et al., 2013). In the present paper, the main goal is to investigate the impact of the nanofluid filled isosceles triangular shaped solar thermal collector with an uneven bottom wall on heat transfer. The literature review revealed that uniform boundary conditions taking into a dynamic model for an isosceles triangular shape enclosure with an uneven bottom wall filled with CuO-water nanofluid has not study yet. This study is carried out numerically and the related results are shown graphically for CuO-water nanofluid to investigate the behaviors of nanofluid and the heat transfer rate.

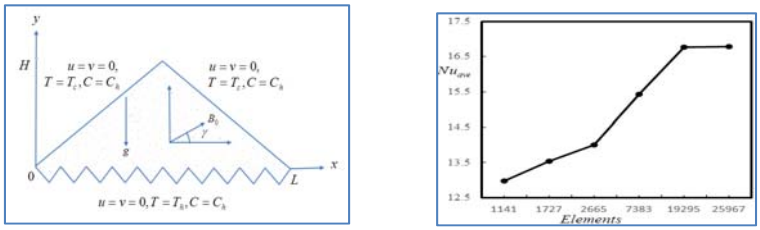

(a) (b)

Figure 1: (a) Schematic of the problem (b) the grid independence test of the enclosure

2. Problem design: pphysical and mathematical modeling

A physical image of the problem is shown in figure 1, where X and Y are the Cartesian coordinates, H is height of cavity and L is the bottom wall length. The horizontal wall represents a thermal plate which can be seen in electronics, electrical and solar equipment applications. So, the condition of the corrugated wall of the isosceles enclosure is modeled as $T = T_n$ whereas, the temperature of both the inclined wall of the enclosure is low as heat goes through it and modeled as $T = T_c$. Initially, it is assumed that nanofluid concentration is kept at low concentration C_c but for $t > 0$, it is assumed as C_n in the entire domain so that $C_n > C_c$. Thermophoresis and Brownian motion are included in absence of chemical reaction and radiation. The base fluid and the solid nanoparticles are thermally equilibrium. Basically, this type of cavity is modeled as a solar thermal collector of which the inclined walls are the glass covers and the corrugated bottom wall is the collector plate. The governing equations (Uddin et al., 2016b, 2017a, 2017b, 2017c) (the continuity, the X-momentum, the Y-momentum, the energy, and the concentration respectively) for nanofluids respectively can be written as:

$$\frac{\partial u}{\partial x}+\frac{\partial v}{\partial y}=0 \tag{1}$$

$$\rho_{nf}\left[\frac{\partial u}{\partial t}+u\frac{\partial u}{\partial x}+v\frac{\partial u}{\partial y}\right]=-\frac{\partial p}{\partial x}+\mu_{nf}\left(\frac{\partial^2 u}{\partial x^2}+\frac{\partial^2 u}{\partial y^2}\right)+\sigma_{nf}B_0^2\left(v\sin(\gamma)\cos(\gamma)-u\sin^2(\gamma)\right) \tag{2}$$

$$\rho_{nf}\left[\frac{\partial v}{\partial t}+u\frac{\partial v}{\partial x}+v\frac{\partial v}{\partial y}\right]=-\frac{\partial p}{\partial x}+\mu_{nf}\left(\frac{\partial^2 v}{\partial x^2}+\frac{\partial^2 v}{\partial y^2}\right)+(\rho\beta)_{nf}g(T-T_c)+(\rho\beta^*)_{nf}g(C-C_c)$$
$$+\sigma_{nf}B_0^2\left(u\sin(\gamma)\cos(\gamma)-v\cos^2(\gamma)\right) \tag{3}$$

$$\frac{\partial T}{\partial t}+u\frac{\partial T}{\partial x}+v\frac{\partial T}{\partial y}=\alpha_{nf}\left(\frac{\partial^2 T}{\partial x^2}+\frac{\partial^2 T}{\partial y^2}\right)+\frac{D_B}{C}\left(\frac{\partial C}{\partial x}\frac{\partial T}{\partial x}+\frac{\partial C}{\partial y}\frac{\partial T}{\partial y}\right)+\frac{D_T}{T}\left[\left(\frac{\partial T}{\partial x}\right)^2+\left(\frac{\partial T}{\partial y}\right)^2\right] \tag{4}$$

$$\frac{\partial C}{\partial t}+u\frac{\partial C}{\partial x}+v\frac{\partial C}{\partial y}=D_B\left(\frac{\partial^2 C}{\partial x^2}+\frac{\partial^2 C}{\partial y^2}\right)+\frac{CD_T}{T}\left(\frac{\partial^2 T}{\partial x^2}+\frac{\partial^2 T}{\partial y^2}\right)+\frac{D_T}{T}\left(\frac{\partial C}{\partial x}\frac{\partial T}{\partial x}+\frac{\partial C}{\partial y}\frac{\partial T}{\partial y}\right) \tag{5}$$

where U and V are the velocities along X, Y coordinates, respectively, p is pressure, g is gravity, T is temperature, T_c is reference temperature, C is concentration and C_c is reference concentration. Here, μ_{nf} is the dynamic viscosity, ρ_{nf} is density, $\alpha_{nf}=K_{nf}/(\rho c_p)_{nf}$ is thermal diffusivity, K_{nf} is thermal conductivity,

$(\rho c_p)_{nf}$ is heat capacity, $(\rho\beta)_{nf}$ is volumetric thermal expansion and $(\rho\beta^*)_{nf}$is the volumetric mass expansion of nanofluid. The last term in the right side of Eg(1-2) are due to the applied magnetic field. The complete calculations of these terms can be found in Uddin et al. (2017c) where, B_0 is the constant magnitude of the uniform applied magnetic field, γ is the inclination angle of the direction of the uniform applied magnetic field to the horizontal axis, σ_{nf} is the electric conductivity of nanofluids. In Eq (1-5), the thermophysical relations of nanofluid that means, σ_{nf}, μ_{nf}, ρ_{nf}, $(\rho c_p)_{nf}$, $(\rho\beta^*)_{nf}$, K_{nf}, D_B and D_T are taken from the study of Uddin et al. (2017c). Also, the appropriate initial and boundary conditions of the isosceles triangular enclosure are as follows:

For $t = 0$, entire domain: $U = V = 0, T = T_c, C = C_h$ and for $t > 0$, on the horizontal corrugated wall: $U = V = 0, T = T_h$, $C = C_h$. Also, on the inclined wall: $U = V = 0, T = T_c, C = C_h$. To describe transport mechanisms in nanofluids, it is worthy to make the conservation equations dimensionless. So, the equations (1-5) can be converted to non-dimensional forms, using the following quantities:

$$U = \frac{uL}{\alpha_{bf}},\ V = \frac{vL}{\alpha_{bf}},\ X = \frac{x}{L},\ Y = \frac{y}{L},\ \theta = \frac{T - T_C}{\Delta T},\ \mathrm{P} = \frac{pL^2}{\rho_{bf}\alpha^2_{bf}},\ \xi = \frac{\alpha_{bf}t}{L^2},\ \Phi = \frac{C - C_C}{\Delta C} \tag{6}$$

where,α_{bf}, L, $\Delta T = T_h - T_c$, $\Delta C = C_h - C_c$, T_c, and C_c are the thermal diffusivity of base fluid, reference length of the geometry, the temperature difference, the nominal concentration difference, reference temperature and reference concentration within the nanofluid, respectively. Introducing the relation (6) into equations (1)-(5), we have dimensionless continuity, momentum in X and Y directions and energy equations respectively as:

$$\frac{\partial U}{\partial X} + \frac{\partial V}{\partial Y} = 0 \tag{7}$$

$$\frac{\partial U}{\partial \xi} + U\frac{\partial U}{\partial X} + V\frac{\partial U}{\partial Y} = -\frac{\rho_{bf}}{\rho_{nf}}\frac{\partial \mathrm{P}}{\partial X} + \frac{\mu_{nf}}{\nu_{bf}\rho_{nf}}\mathrm{Pr}\left(\frac{\partial^2 U}{\partial X^2} + \frac{\partial^2 U}{\partial Y^2}\right) + \frac{\sigma_{nf}}{\sigma_{bf}}\mathrm{Pr}\,Ha^2\left(V\sin(\gamma)\cos(\gamma) - U\sin^2(\gamma)\right) \tag{8}$$

$$\frac{\partial V}{\partial \xi} + U\frac{\partial V}{\partial X} + V\frac{\partial V}{\partial Y} = -\frac{\rho_{bf}}{\rho_{nf}}\frac{\partial \mathrm{P}}{\partial Y} + \frac{\mu_{nf}}{\nu_{bf}\rho_{nf}}\mathrm{Pr}\left(\frac{\partial^2 V}{\partial X^2} + \frac{\partial^2 V}{\partial Y^2}\right) + \frac{(\rho\beta)_{nf}}{\beta_{bf}\rho_{nf}}Ra_T\,\mathrm{Pr}\,\theta + Ra_C\,\mathrm{Pr}\,\Phi + \frac{\sigma_{nf}}{\sigma_{bf}}\mathrm{Pr}\,Ha^2\left(U\sin(\gamma)\cos(\gamma) - V\cos^2(\gamma)\right) \tag{9}$$

$$\frac{\partial \theta}{\partial \xi} + U\frac{\partial \theta}{\partial x} + V\frac{\partial \theta}{\partial y} = \frac{\alpha_{nf}}{\alpha_{bf}}\left(\frac{\partial^2 \theta}{\partial X^2} + \frac{\partial^2 \theta}{\partial Y^2}\right) + \frac{1}{Le}\left(\frac{\partial \Phi}{\partial X}\frac{\partial \theta}{\partial X} + \frac{\partial \Phi}{\partial Y}\frac{\partial \theta}{\partial Y}\right) + \frac{\mathrm{Pr}\,N_{TBT}}{Sc}\left(\left(\frac{\partial \theta}{\partial X}\right)^2 + \left(\frac{\partial \theta}{\partial Y}\right)^2\right) \tag{10}$$

$$\frac{\partial \Phi}{\partial \xi} + U\frac{\partial \Phi}{\partial X} + V\frac{\partial \Phi}{\partial Y} = \frac{\mathrm{Pr}}{Sc}\left(\frac{\partial^2 \Phi}{\partial X^2} + \frac{\partial^2 \Phi}{\partial Y^2}\right) + \frac{\mathrm{Pr}}{Sc}N_{TBTC}\left(\frac{\partial^2 \theta}{\partial X^2} + \frac{\partial^2 \theta}{\partial Y^2}\right) + \frac{\mathrm{Pr}}{Sc}N_{TBT}\left(\frac{\partial \Phi}{\partial X}\frac{\partial \theta}{\partial X} + \frac{\partial \Phi}{\partial Y}\frac{\partial \theta}{\partial Y}\right) \tag{11}$$

where $\mathrm{Ra}_T = \frac{L^3\beta_{\mathrm{bf}}\,g\Delta T}{V_{\mathrm{bf}}\,\alpha_{\mathrm{bf}}}$, $\mathrm{Ra}_C = \frac{L^3 g\Delta C(\rho\beta^*)_{\mathrm{nf}}}{V_{\mathrm{bf}}\alpha_{\mathrm{bf}}\rho_{\mathrm{nf}}}$, $Le = \frac{K_{\mathrm{bf}}C_C}{(\rho C_P)_{\mathrm{bf}}D_B\Delta C}$, $\mathrm{Pr} = \frac{V_{\mathrm{bf}}}{\alpha_{\mathrm{bf}}}$, $\mathrm{Ha}^2 = \frac{L^2\sigma_{\mathrm{bf}}B_0^2}{V_{\mathrm{bf}}\,\rho_{\mathrm{bf}}}$, $N_{TBT} = \frac{D_T}{D_B}\frac{\Delta T}{T_C}$, $N_{TBTC} = \frac{D_T}{D_B}\frac{\Delta T}{\Delta C}\frac{C_C}{T_C}$ and $\mathrm{Sc} = \frac{\mu_{\mathrm{bf}}}{\rho_{\mathrm{bf}}D_B}$ is the local thermal Rayleigh number, local modified Rayleigh number, modified Lewis number, Prandtl number, Hartmann number, dynamic thermo-diffusion parameter, dynamic diffusion parameter, and the Schmidt number respectively. Now, also, the initial and boundary conditions in the dimensionless form for the present problem along with the above-stated model can be written as: for $\xi = 0$, entire domain: $U = V = 0$, $\theta = 0$, $\Phi = 1$, and for $\xi > 0$, on the horizontal corrugated wall: $U = V = 0$, $\theta = 1$, $\Phi = 1$. Also, on the inclined walls: $U = V = \theta = 0$, $\Phi = 1$.

3. Computational procedures

The Galerkin weighted residual scheme of finite element method (FEM) is applied to solve Eq (7)-(11) together with dimensionless initial and boundary conditions. The step by step procedures of this numerical method over the conservation equations of the present problem are available in Uddin and Rahman (2018). In the present study, a partial differential equation solver with MATLAB interface is used to solve the whole system. Also, to surety a grid- independent solution for C_uO -water nanofluid, an extensive mesh testing procedure has been steered for $\mathrm{Ra}_c = 10^4$, $\mathrm{Ra}_T = 10^6$, $Ha = 100$, $\gamma = 0^\circ$,$\emptyset = 0.05$, $d_{\mathrm{p}} = 10nm$, $\mathrm{n} = 3$ and $\xi = 1$ in an isosceles triangular cavity. Six different non-uniform grid systems such as: 1141, 1727, 2665, 7383, 19295 and 25967 for the cavity have been tested. The numerical simulation has performed in Nu_{ave} at

the heated wall for the abovementioned grids to understand the grid fineness as shown in Figure 1(b). The scale of Nu_{ave} for 19295 elements shows a similar result with that for the elements of 25967. Hence, from grid size of 19295 is found to meet the requirement of the grid independence study.

Table 1: *Comparisons of the present code with that of the results of Saghir et al. and Ho et al..*

Studies	Nu_{ave}		
	$\emptyset = 1\%$	$\emptyset = 2\%$	$\emptyset = 3\%$
Saghir et al.	32.2037	31.0905	29.0769
Ho et al.	31.8633	31.6085	28.2160
Present result	32.1900	31.0354	28.9580

Also, a code validation test is performed before displaying and analyzing the results. We have tested the precision of current numerical code by associating the numerically replicated outcomes of Saghir et al. (2016) and the experimental results of Ho et al. (2010) which is shown in Table 1. In this case, for the present code is utilized to validate the study of Saghir et al. (2016). The results were presented in the form of an experimental expression of the average Nusselt number (Nu_{ave})as $Nu_{\mathrm{ave}} = 0.069(Pr_{\mathrm{nf.h}}/Pr_{\mathrm{nf}})^{0.333}(\beta_{\mathrm{nf.h}}/\beta_{\mathrm{nf}})^{0.404}$, where, $\beta_{\mathrm{nf.h}}/\beta_{\mathrm{nf}}$ is the ratio of the Prandtl number at the hot temperature to the Prandtl number at the mean temperature of $26^{\circ}\ C$ and the temperature change of $12^{\circ}\ C$. Also, $\beta_{\mathrm{nf.h}}/\beta_{\mathrm{nf}}$, is the ratio of thermal expansions between at the hot temperature and mean temperature. The above relation is used to compare the results. The results in Nu_{ave} for different nanoparticle volume fraction is displayed in Table 1. It is seen that present numerical code has anticipated the standard results with an upright concord which gives confidence on the present code.

4. Results and discussions

The properties of copper-oxide and water is used for results. The thermophysical properties of copper-oxide nanoparticle and kerosene are available in Uddin et al. (2017b). Let us consider $\Delta T = 10K$, $\Delta C = 0.01$, $T_c = 300\mathrm{K}$ $C_c = 1$, $d_p = 10\mathrm{nm}$, $n = 3$ and $\emptyset = 0.05$, the physical parameters entered into the equations (7)-(11) for copper oxide -water nanofluids are as follows: $Le = 3.82 \times 10^5$, $Sc = 26111$, $D_B = 3.8525 \times 10^{-11}$,$D_T = 8.725 \times 10^{-12}$, $N_{TBTC} = 0.75495$ and $N_{TBT} = 0.0075495$. The other parameters of the problem are varied for analyzing the results. The ratio of the buoyancy parameters $\mathrm{Ra_c}$and $\mathrm{Ra_T}$has been fixed to 100. From Figure 2(a), it is observed that magnetic field inclination angle significantly strikes and controls the flow field and thermal field. The patterns of the streamlines and isotherms are directed to the directions of the magnetic field. This is due to the hydro-magnetized nanoparticles which have monoclinic structure and ferromagnetic behavior. The vortices inside the enclosure oppositely rotate each other and the pattern of the rotations fully shaped according to the directions of the magnetic field. As the magnetic field inclination angle is increased, the strengths of the streamlines and isotherms are enhanced, the intensities of the rotations of the flow inside the enclosure upsurge and the number of vortices and the thermal plumes of isotherms step-up. The most distorted streamlines and isotherms can be observed for $\gamma = 90^0$which indicates maximum heat transfer. Figure 3 represents the average Nusselt number versus different values of the (a) Rayleigh number (b) Hartmann number, (c) magnetic field inclination angle (d) diameter of particle, (e) shape of particle and (f) time. As can be seen that the heat transfer rate is significantly higher for nanofluid than that of base fluid. From Figure 3(a), we have seen that the average Nusselt number is increased when the thermal Rayleigh number is increased. For the changes of the lower values of the thermal Rayleigh number, the average Nusselt is not changed for nanofluid whereas, the noticeable effect can be observed for base fluid. This means that more buoyancy force is needed to enhance the heat transfer for nanofluid than that of base fluid. Also, as nanoparticle volume faction increases, more buoyancy force needs to instigate the heat transfer. It can also be seen that 10^5 is the critical Rayleigh number for base fluid whereas $5 \times 10^5$is the critical Rayleigh number for nanofluid of having 5% nanoparticle. As nanoparticle volume fraction increases, the value of the critical Rayleigh number increases. The effect of the magnetic field for nanofluid is seriously distinguishable than that of the base fluid which is shown in Figure 3(b). decreases gradually throughout the values of the magnetic field parameter for the base fluid whereas for nanofluid, it decreases significantly for Ha=0-100 and then it becomes level out, reach a stable state.

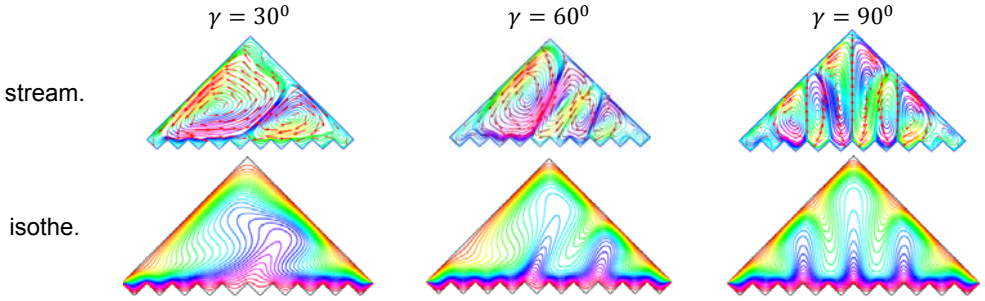

Figure 2: Effect of magnetic field inclination angle on streamlines (1st row) and isotherms (2nd row) for $Ra_T = 10^6$, $d_p = 10nm$, $\emptyset = 0.05$, $Ha = 100$, $n = 3$ *at* $\xi = 1$.

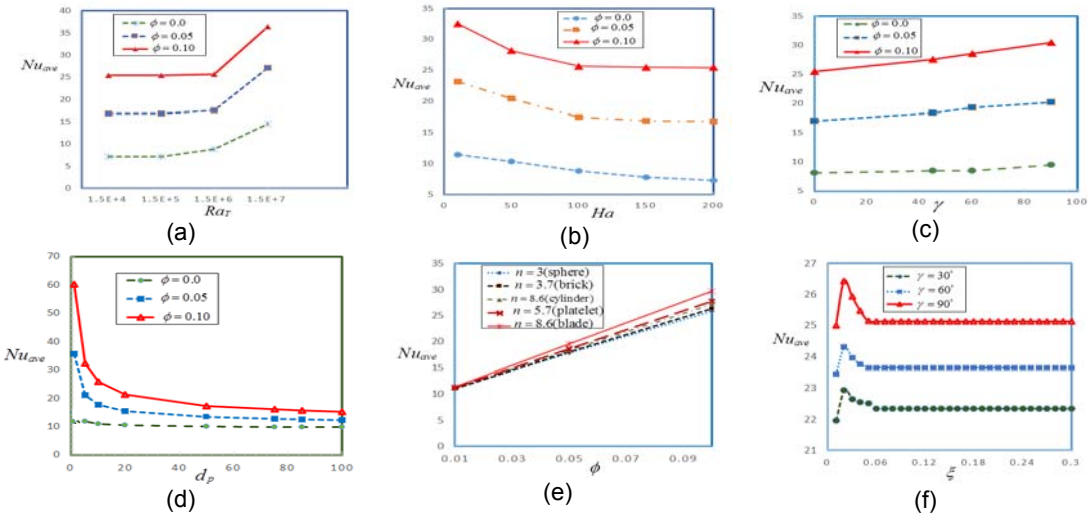

Figure 3: Average Nusselt number versus different values of (a) Rayleigh number (b) Hartmann number, (c) magnetic field inclination angle (d) diameter of particle, (e) shape of particle and (f) time for the fixed values of $\emptyset = 0.05$, $Ha_T = 1.7 \times 10^6$, $d_p = 10nm$, $Ha = 100$, $n = 3$, $\gamma = 0^0$ *and* $\xi = 1$

From Figure 3(c), it shows that the average Nusselt number enhances with the increment of magnetic field inclination angle. The increasing trend of the average Nusselt number is very sharp for nanofluid for 0^0-90^0 whereas, for base fluid, it is steady for 0^0-55^0 and sharply increased for approximately, 55^0-90^0. Also, the nanoparticle diameter effects on the heat transfer are shown in Figure 3(d). As can be seen that the heat transfer decreases with the increase in the size of the nanoparticle diameter. The striking decreasing trend on the average Nusselt number can be observed for the diameter of 1-55 nm. It is important to note that as the nanoparticle volume fraction increases, this decreasing trend of the heat transfer for different diameter of the nanoparticle enhances. So, to get better performance, it is recommended that the size of the solid particles should be small as much as possible. Different shapes effects of nanoparticle on the heat transfer are observed in Figure 3(e). Different shapes of the nanoparticle are calculated using the shape factor. We have found that as the shape factor increases, the heat transfer increases. The blade shape exhibits the highest heat transfer rate whereas the spherical shape of nanoparticle shows lowest heat transfer. From the lower to higher for shapes can be listed respective as spherical, brick, cylindrical, platelet and blade. The heat transfer rate for different shapes can be observed clearly if the nanoparticle volume fraction is more than 3%. Figure 3(f) represents the evolution of the average Nusselt number for different times. It is observed that in the initial periods of time, the average Nusselt number fluctuates and after certain periods of time, it becomes plateau. This indicates that nanoparticles and the base fluid are in an unstable state initially and after sometimes, they become equilibrium. Also, the heat transfer is significantly higher when the magnetic field inclination angle is 90^0.

5. Conclusions

The natural convective heat transfer inside an isosceles triangular enclosure with the uneven bottom wall has been simulated numerically. Numerical results demonstrate that the presence of magnetic field is playing a key role to control direction of the flow and the heat transfer. The nanoparticles and the base fluid take time and need strong buoyancy force to be a thermal equilibrium. Initially, the heat transfer fluctuates and after that it becomes stable. After a certain value of the thermal Rayleigh number, the heat transfer rate of an application is an increasing function of thermal Rayleigh number, nanoparticle volume fraction, and magnetic field inclination angle. Also, it is a decreasing function of the diameter of nanoparticle and the applied magnetic field.

References

Billah M.M., Rahman M.M., Razzak M.A., Saidur R., Mekhilef S., 2013, Unsteady Buoyancy-driven Heat Transfer Enhancement of Nanofluids in an Inclined Triangular Enclosure, International Communications in Heat and Mass Transfer, 49, 115-127, DOI: 10.1016/j.icheatmasstransfer.2013.09.006

Bondareva N.S., Sheremet M.A., Pop I., 2015, Magnetic Field Effect on the Unsteady Natural Convection in a Right-angle Trapezoidal Cavity Filled with a Nanofluid: Buongiorno's Mathematical model, International Journal of Numerical Methods for Heat & Fluid Flow, 25(8), 1924-1946.

Buongiorno J., 2006, Convective Transport in Nanofluids, Journal of Heat Transfer, 128(3), 240-250.

Colangelo G., Favale E., De Risi A., Laforgia D., 2013, A new Solution for Reduced Sedimentation Flat Panel Solar Thermal Collector Using Nanofluids, Applied Energy, 111, 80-93.

Ghasemi B., Aminossadati S.M., 2010, Brownian Motion of Nanoparticles in a Triangular Enclosure with Natural Convection, International Journal of Thermal Sciences, 49(6), 931-940.

Haichao L., Xiaona S., Yongwei G., 2017, Study on Cooling Characteristics of Water-based Carbon Nanotube Nanofluids for Internal Combustion Engines, Chemical Engineering Transactions, 59, 1075-1080.

Ho C.J., Liu W.K., Chang Y.S., Lin C.C., 2010, Natural Convection Heat Transfer of Alumina-water Nanofluid in Vertical Square Enclosures: An Experimental Study, International Journal of Thermal Sciences, 49(8), 1345-1353.

Lai F.H., Yang Y.T., 2011, Lattice Boltzmann Simulation of Natural Convection Heat Transfer of Al2O3/water Nanofluids in a Square Enclosure, International Journal of Thermal Sciences, 50(10), 1930-1941.

Saghir M.Z., Ahadi A., Mohamad A., Srinivasan S., 2016, Water Aluminium Oxide Nanofluid Benchmark Model, International Journal of Thermal Sciences, 109, 148-158.

Ting Z., Jianhong T., 2017, Application of Nano-micronized Sio to Electrostatic Shielding Materials, Chemical Engineering Transactions, 62, 121-126, DOI:10.3303/CET1762021.

Tiwari R.K., Das M.K., 2007, Heat Transfer Augmentation in a Two-sided Lid-driven Differentially Heated Square Cavity Utilizing Nanofluids, International Journal of Heat and Mass Transfer, 50(9-10), 2002-2018.

Tzeng S.C., Liou J.H., Jou R.Y., 2005, Numerical Simulation-aided Parametric Analysis of Natural Convection in a Roof of Triangular Enclosures, Heat Transfer Engineering, 26(8), 69-79.

Uddin M.J., Al Kalbani K.S., Rahman M.M., Alam M.S., Al-Salti N., Eltayeb I., 2016a, Fundamentals of Nanofluids: Evolution, Applications and New Theory, International Journal of Biomathematics and Systems Biology, International Journal of Biomathematics and Systems Biology, 2(1), 1-32.

Uddin M.J., Alam M.S., Al-Salti N., Rahman M.M., 2016b, Investigations of Natural Convection Heat Transfer in Nanofluids Filled Horizontal Semicircular-annulus Using Nonhomogeneous Dynamic Model, American Journal of Heat and Mass Transfer, 3(6), 425-452.

Uddin M.J., Alam M.S., Rahman M.M., 2017b, Natural Convective Heat Transfer Flow of Nanofluids Inside a Quarter-circular Enclosure Using Nonhomogeneous Dynamic Model, Arabian Journal for Science and Engineering, 42(5), 1883-1901.

Uddin M.J., Rahman M.M., 2017, Numerical Computation of Natural Convective Heat Transport Within Nanofluids Filled Semi-circular Shaped Enclosure Using Nonhomogeneous Dynamic Model, Thermal Science and Engineering Progress, 1, 25-38.

Uddin M.J., Rahman M.M., 2018, Finite Element Computational Procedure for Convective Flow of Nanofluids in an Annulus, Thermal Science and Engineering Progress, 6, 251-267.

Uddin M.J., Rahman M.M., Alam M.S., 2017c, Analysis of Natural Convective Heat Transport in Homocentric Annuli Containing Nanofluids with an Oriented Magnetic Field Using Nonhomogeneous Dynamic Model, Neural Computing and Applications, 1-20, DOI: 10.1007/s00521-017-2905-z.

Wen D., Ding Y., 2004, Experimental Investigation into Convective Heat Transfer of Nanofluids at the Entrance Region Under Laminar Flow Conditions, International Journal of heat and Mass Transfer, 47(24), 5181-5188, DOI: 10.1016/j.ijheatmasstransfer.2004.07.012